Published in final edited form as:
J Proteome Res. 2011 January 7; 10(1): 241–248. doi:10.1021/pr1008898.

Quantification of Cholesterol-Metabolizing P450s CYP27A1 and CYP46A1 in Neural Tissues Reveals a Lack of Enzyme-Product Correlations in Human Retina but not Human Brain

Wei-Li Liao[†,§], **Gun-Young Heo**[‡], **Nathan G. Dodder**[§,#], **Rachel E. Reem**[‡], **Natalia Mast**[‡], **Suber Huang**[‡,∫], **Pier Luigi DiPatre**[¶,&], **Illarion V. Turko**[*,†,§], and **Irina A. Pikuleva**[*,‡]
Institute for Bioscience and Biotechnology Research, Rockville, Maryland 20850, Analytical Chemistry Division, National Institute of Standards and Technology, Gaithersburg, Maryland 20899, Department of Ophthalmology and Visual Sciences, Case Western Reserve University and University Hospitals, Cleveland, Ohio 44106, and Department of Pathology, University of Texas Medical Branch, Galveston, Texas 77555

Abstract

The cytochrome P450 enzymes (CYP or P450) 46A1 and 27A1 play important roles in cholesterol elimination from the brain and retina, respectively, yet they have not been quantified in human organs because of their low abundance and association with membrane. Based on our previous development of a multiple reaction monitoring (MRM) workflow for measurements of low abundance membrane proteins, we quantified CYP46A1 and CYP27A1 in human brain and retina samples from four donors. These enzymes were quantified in the total membrane pellet, a fraction of the whole tissue homogenate, using ^{15}N-labled recombinant P450s as internal standards. The average P450 concentrations per mg of total tissue protein were 345 fmol of CYP46A1 and 110 fmol of CYP27A1 in the temporal lobe, and 60 fmol of CYP46A1 and 490 fmol of CYP27A1 in the retina. The corresponding P450 metabolites were then measured in the same tissue samples and compared to the P450 enzyme concentrations. Investigation of the enzyme-product relationships and analysis of the P450 measurements based on different signature peptides revealed a possibility of retina-specific post-translational modification of CYP27A1. The data obtained provide important insights into the mechanisms of cholesterol elimination from different neural tissues.

Keywords

CYP27A1; CYP46A1; absolute quantification; multiple reaction monitoring; mass spectrometry; membrane protein; human brain; human retina

[*]To whom correspondence should be addressed. Dr. Illarion V. Turko, 9600 Gudelsky Dr., Rockville, MD 20850. turko@umbi.umd.edu or Dr. Irina A. Pikuleva, 2085 Adelbert Road, room 303, Cleveland, OH 44106. iap8@case.edu.
[†]Institute for Bioscience and Biotechnology Research.
[§]Analytical Chemistry Division, National Institute of Standards and Technology.
[‡]Department of Ophthalmology and Visual Sciences, Case Western Reserve University and
[∫]University Hospitals.
[¶]Department of Pathology, University of Texas Medical Branch.
[#]Current address: Southern California Coastal Water Research Project, Costa Mesa, CA 92626.
[&]Current address: Scott and White Clinic, Neuroscience Institute, Temple TX 76508

Supporting Information Available: Supplemental Figures and Table. This information is available free of charge via the Internet at http://pubs.acs.org/.

Introduction

Cholesterol is essential for life in mammals, yet if chronically in excess it becomes a risk factor for cardiovascular and Alzheimer's diseases and possibly age-related macular degeneration.[1–3] The mechanisms that control cholesterol levels vary depending on the organ but all comprise cholesterol hydroxylation, an enzymatic process that initiates cholesterol removal.[4] Cholesterol hydroxylation is especially important for the maintenance of cholesterol homeostasis in the brain, where the conversion to 24S-hydroxycholesterol, catalyzed by the cytochrome P450 enzyme CYP46A1, represents the major mechanism of cholesterol elimination.[5–7] In the brain, cholesterol is also metabolized to 27-hydroxycholesterol and pregnenolone by CYP27A1 and CYP11A1, respectively. However, under normal conditions these enzymatic reactions are quantitatively less important than cholesterol 24S-hydroxylation.[8] The brain is a part of the central nervous system, which also includes the retina, a thin layer of image-processing neuronal cells that line the back of the eye. Recent work has investigated cholesterol elimination from the retina.[9–12] Evidence suggests that the two neural tissues, the brain and retina, have distinct mechanisms of enzymatic cholesterol elimination.[13] Recently, we measured the levels of different cholesterol metabolites in samples from human donors and found that in the retina cholesterol is predominantly hydroxylated at position 27, not position 24 as in the brain, and the major cholesterol metabolite, 5-cholestenoic acid, is a derivative of 27-hydroxycholesterol, rather than 24S-hydroxycholesterol. We also found that retinal concentrations of 5-cholestenoic acid vary significantly in human subjects, raising a question as to whether the expression of CYP27A1 varies as well.[13] However, at the time neither CYP27A1 nor CYP46A1 had been quantified in human tissues.

Multiple reaction monitoring (MRM) assays allow the simultaneous quantification of multiple proteins in complex biological samples. This approach relies on liquid chromatography coupled to triple quadrupole mass spectrometry (LC-MS/MS) and has successfully been used for the analysis of biomarkers and the determination of protein modifications in cell lysates and human plasma.[14–17] However, the application of MRM assays to the direct measurement of membrane proteins is more recent[18–20] and still represents a challenge. Cholesterol-metabolizing P450s are low abundance membrane proteins; therefore, MRM assays for these P450s require optimization of the tissue processing procedure in addition to optimization of the instrumental parameters. Previously, we developed a protocol for quantification of low fmol levels of CYP11A1 per mg of tissue protein, and suggested that this protocol can be used for the measurement of other membrane proteins.[20] In the present work, we have confirmed the applicability of this protocol and measured brain and retinal concentrations of microsomal CYP46A1 and mitochondrial CYP27A1. Protein quantification was carried out on specimens from four donors and the results support the notion that cholesterol elimination from the retina is indeed different from that in the brain. We also measured the concentrations of the P450 products 24S-hydroxycholesterol, 27-hydroxycholesterol and 5-cholestenoic acid in the same donor samples. Analysis of the enzyme-product relationships revealed a lack of enzyme-product correlations in human retina but not human brain. This unexpected finding suggests retina-specific post-translational modification of CYP27A1.

Experimental Section

Materials

Ammonium chloride (^{15}N, 99 %), [25,26,26,26,27,27,27-$^{2}H_7$]24-hydroxycholesterol, [26,26,26,27,27-$^{2}H_5$]27-hydroxycholesterol, 5-cholestenoic acid and 5-cholenic acid-3β-ol were purchased from Cambridge Isotope Laboratories (Andover, MA). Unlabeled 24S-hydroxycholesterol and 27-hydroxycholesterol were from Avanti Polar Lipids, Inc

(Alabaster, AL). The *DC* Protein Assay kit was from Bio-Rad Laboratories (Hercules, CA). Complete, EDTA-free, cocktail of protease inhibitors was from Roche Diagnostics (Indianapolis, IN). Sequencing grade modified trypsin was obtained from Promega Corp. (Madison, WI). All other chemicals were purchased from Sigma-Aldrich (St. Louis, MO).

Protein Standards

Recombinant human CYP27A1 and CYP46A1 were expressed and purified as described. [21, 22] To obtain ^{15}N-labeled proteins, *Escherichia coli* cells GC5 were co-transformed with the expression construct for specific P450 and pGro7 vector (Takara Bio Inc., Japan) containing chaperones GroEL and GroES. Subsequent expression followed the procedure of Marley et al.[23] Briefly, overnight cultures were diluted 100-fold with 3L of Terrific Broth medium and grown by shaking (250 rpm) at 37°C until $O.D_{600}$ reached 0.6. Cultures were then washed twice with 1L of M9 minimal media salt solution followed by incubation in 1L of M9 minimal media containing 1 g/L of $^{15}NH_4Cl$ as the sole nitrogen source and 0.5 mM δ-aminolevulinic acid. Expression of P450s and chaperones was induced by 1 mM isopropyl β-D-thiogalatopyranoside and 0.18 g/ml L arabinose, respectively, and proceeded for 72 hours by shaking at 210 rpm. CYP27A1 was expressed at 29.5 °C whereas CYP46A1 was expressed at 26.5 °C. Purification of ^{15}N-labeled P450s was similar to that of the unlabeled proteins. The P450 concentration was assessed by the CO-reduced difference spectrum using an absorption coefficient of 91 $mM^{-1}cm^{-1}$ for the absorbance difference between 450 and 490 nm.[24]

In-Solution Digestion

Recombinant ^{15}N-labeled and unlabeled P450s (100 pmol each) were digested in 25 mM NH_4HCO_3 using 0.1 μg of trypsin. The mixtures were incubated for 15 h at 37 °C and stored in aliquots at −20 °C.

Determination of ^{15}N Incorporation

The percent incorporation of ^{15}N in the recombinant P450 was determined at the peptide level. Simulated isotopic distributions with varying percent of ^{15}N incorporation were generated for multiple tryptic ^{15}N-labeled peptides from each protein, using the OrgMassSpecR computer program (http://orgmassspecr.r-forge.r-project.org). These simulations were then compared to the experimental precursor ion mass spectra acquired on a 4700 Proteomics Analyzer (Applied Biosystems, Framingham, MA) to determine the best match and therefore the ^{15}N incorporation.

Human Tissues

Human tissue use conformed to the Declaration of Helsinki and institutional reviews at the University of Texas Medical Branch and Case Western Reserve University. Brain and eye specimens were obtained from de-identified donors following informed consent of the respective families. Demographic information on the donors and pertinent medical history are summarized in the Supporting Information (Table S1). Samples of gray matter from the temporal lobe were obtained during autopsy at the University of Texas Medical Branch 9–11 h after death. These samples were rinsed in cold 0.9% NaCl, blotted, flash frozen in liquid nitrogen, and stored at −80 °C. Eyes were acquired through the Cleveland Eye Bank and dissected within 10–14 hrs after death. The anterior segment was removed, and fundus photos were taken to confirm the absence of retinal pathology. Thereafter, the neural retina was isolated, flash-frozen in liquid nitrogen and stored at −80 °C until analyzed.

Processing of the Human Brain and Retina

Extraction of the target proteins followed a previously described procedure designed for the absolute quantification of membrane proteins.[20] The steps included: (i) homogenization of the biological sample in a trypsin compatible buffer (25 mM NH_4HCO_3); (ii) use of 2% SDS to measure the total protein concentration in the tissue homogenate; (iii) use of the total membrane pellet obtained after the 153 000*g* centrifugation of the tissue homogenate, and (iv) use of trypsin-compatible detergents. While all these steps are important, the key innovation was the use of the total membrane pellet,[20] through which it had been possible to detect mitochondrial cytochrome P450 11A1 (CYP11A1) at 7 fmol/mg of tissue protein. In the present work, each tissue was placed in 25 mM NH_4HCO_3 and homogenized by sonication at 30 W using three 10 s continuous cycles (Sonicator 3000, Misonix Inc., Farmingdale, NY). The total protein concentration was measured in the presence of 2% SDS using the *DC* protein Assay kit and bovine serum albumin as a standard. The homogenates were then aliquoted into 1 mg-portions of the total tissue protein *per* tube. One set of tubes was frozen at −80 °C, whereas the other set was subjected to centrifugation at 153 000*g* for 30 min. The resulting pellet was frozen at −80 °C. Thus, two types of fractions were obtained and used for subsequent measurements: the whole tissue homogenate and the total membrane pellet. During the following processing, each fraction was supplemented with 0.2% sodium cholate in 25 mM NH_4HCO_3 and an exact known amount of the ^{15}N-labeled internal standards, ^{15}N-CYP27A1 and ^{15}N-CYP46A1. The samples were heated at 90 °C for 5 min, cooled to room temperature, and treated with trypsin type IX-S from porcine pancreas (Sigma-Aldrich, catalog number T0303) for 15 h at 37 °C. The substrate/trypsin ratio was 50:1 (w/w). After trypsinolysis, the samples were centrifuged at 153 000*g* for 30 min, and the supernatants were transferred to new tubes. Each supernatant was then treated with 0.5% TFA for 30 min at 37 °C and centrifuged again at 153 000*g* for 30 min. The supernatants from the second centrifugation were transferred to new tubes again, mixed with an equal volume of acetonitrile, and dried using a Vacufuge (Eppendorf AG, Hamburg, Germany).

LC-MS/MS Analysis

Instrumental analyses were performed on a hybrid triple quadrupole/linear ion trap mass spectrometer (4000 QTRAP, ABI/MDS-Sciex) coupled to an Eksigent nanoLC-2D system (Dublin, CA). Peptide separations were performed with a PicoFrit (75 μm ID/10 μm tip ID, New Objective) column self-packed to a bed length of 12 cm with Reprosil-Pur 120 C18-AQ, 3 μm resin (Dr. Maisch GmbH, Germany). Peptides were eluted over a 42 min-gradient from 13% to 31% acetonitrile, containing 0.1% formic acid and at a flow rate of 300 nL/min. The column effluent was continuously directed into the nanospray source of the mass spectrometer. All acquisition methods used the following parameters: an ion spray voltage of 2100 V, curtain gas of 30 psi, source gas of 9 psi, interface heating temperature of 170 °C, declustering potential of 76 V for +2 precursor ions and 65 V for +3 precursor ions, collision energy of 30 V for +2 precursor ions and 22 V for +3 precursor ions, and collision cell exit potential of 16 V for +2 precursor ions and 13V for +3 precursor ions. The dwell time for all transitions was 40 ms.

Quantitative Analysis and Validation

Protein concentrations were calculated from the ratio of the light and heavy MRM peak areas multiplied by the known amount of ^{15}N-labeled internal standard of P450 spiked into the sample prior to the digestion. The mass spectrometer monitored three transitions per peptide. The identities of the measured peptides were confirmed based on two parameters of the internal standard which was run under the same conditions: (1) the retention time of the three MRM peaks from a given peptide and (2) the ratio among the three MRM peaks. The selection of the MRM transitions is described in Results and Discussion. The three

transitions from each peptide were treated as independent measurements, each resulting in a concentration value expressed as pmol of quantified protein per mg of total tissue protein. The mean and standard deviation for the consensus protein concentrations were calculated by treating the three transitions for each of the target peptides and the three experimental replicates all as independent measurements.

Quantification of Sterols

Sterols were quantified by isotope dilution gas chromatography-mass spectrometry (GC-MS) as described previously.[13] The internal standards were [25,26,26,26,27,27,27-$^{2}H_{7}$]cholesterol, [25,26,26,26,27,27,27-$^{2}H_{7}$]24-hydroxycholesterol, [26,26,26,27,27-$^{2}H_{5}$]27-hydroxycholesterol, and 5-cholenic acid-3β-ol. The following ions (m/z) were monitored: 368 (cholesterol), 375 (cholesterol-D_{7}), 145 (24-hydroxycholesterol); 152 (24-hydroxycholesterol-D_{7}), 417 (27-hydroxycholesterol), 422 (27-hydroxycholesterol-D_{5}), 331 (5-cholenic acid-3β-ol), and 373 and 412 (5-cholestenoic acid).

Results and Discussion

Characterization of ^{15}N-Labeled P450s

Studies by our group and others indicate that, for MRM measurements, labeled protein internal standards perform better than signature labeled peptides.[20, 25–27] Protein standards reduce variance due to incomplete digestion and/or missed-cleavage, which is especially important for quantification of membrane proteins since their digestion can be inefficient. Also, labeled proteins provide a broad selection of peptides for quantification, allow the detection of posttranslational modifications, and distinguish between various protein isoforms in a complex biological sample. Therefore, in the present study we continued to use ^{15}N-labeled proteins as internal standards for the MRM measurements. To ensure accurate quantification, we first evaluated the isotopic incorporation in the internal standards as described previously.[20] Briefly, purified ^{15}N-CYP27A1 and ^{15}N-CYP46A1 were digested in solution with trypsin and mass spectra of the digests were acquired on a 4700 MALDI-TOF/TOF (Applied Biosystems, Framingham, MA) operated in the single stage MS mode. Multiple peptides from each protein were analyzed for their ^{15}N incorporation by simulating the isotopic distributions from 92% to 100% ^{15}N incorporation, with 1% increments. These simulations were then compared to the experimental spectra to determine the best fit. The same labeling efficiencies were observed in multiple peptides from each protein. Figure 1 shows experimental spectra for representative peptides and their closest simulated isotopic distribution. This comparison shows that the ^{15}N-labeling efficiency was approximately 99% for ^{15}N-CYP27A1 and 95% for ^{15}N-CYP46A1.

Selection and Validation of the MRM Transitions

We used the previously described procedure[20] to identify the optimal signature peptides and optimal transitions for the target proteins. Briefly, the optimal peptides were determined by first monitoring the +2 and +3 precursor ion charge states for each theoretically possible tryptic peptide in unlabeled recombinant CYP27A1 and CYP46A1. Next, for the detected peptides, the +2 charge precursor ions with the corresponding +1 charge fragment ions, and the +3 charge precursor ions with the corresponding +1 and +2 charge fragment ions, were measured in MRM mode. We used the following rules to select the target peptides: (1) methionine- and cysteine-containing peptides were excluded due to the existence of various natural oxidation entities, which could introduce variations in the quantification; (2) putative membrane-associated peptides [28, 29] were excluded; (3) only peptides with zero missed cleavages and molecular weights between 700 Da and 2500 Da were selected; (4) only peptides whose uniqueness was verified by a tblastn search of the human genome (http://blast.ncbi.nlm.nih.gov/Blast.cgi) were selected; and (5) only *b*- and *y*-ions with *m/z*

values greater than the precursor *m/z* were selected because these fragments tend to be more intense and there is less noise in this region of the spectrum. These experiments allowed us to select four signature peptides per P450 and the three most intense MRM transitions per each peptide (Table 1).

The signal intensities of the twelve MRM transitions for each target protein were measured in tissue samples spiked with the ^{15}N-labeled P450s. Tables 2 and 3 show that only two of the four CYP27A1 signature peptides were recovered in the temporal lobe and three of the four CYP46A1 peptides were found in the retina. The peak areas from the labeled internal standards in the biological sample were always smaller than those of the internal standards digested in pure solution alone, leading to a decrease in the abundance of certain peptides below the level of confident detection. This lower recovery of the labeled peptides implies that the efficiency of the tryptic hydrolysis of membrane proteins in biological samples was not identical to that in pure solution. It is also possible that hydrophobic peptides from the membrane proteins adhere to lipid membranes and have reduced extraction efficiency. In either case, the reduced peptide recovery should equally affect the ^{15}N-labeled standard and unlabeled analyte, and should not influence the results of the quantification.

The accuracy of protein quantification could also be affected by non-specific interference from the biological sample that overlaps with the selected transitions.[15, 20] To validate the selected transitions, the relative ratios of the three transitions for every pair of labeled and none-labeled peptides were evaluated. Figure 2 shows the extracted ion chromatograms and MRM spectra of the transitions monitored for representative peptides from ^{15}N-CYP27A1 and CYP27A1 in the retina. The full set of data for all transitions monitored for CYP27A1 and CYP46A1 in the temporal lobe and retina is in the Supporting Information (Figure S1 and Figure S2) and demonstrate the absence of any interference due overlap from to the biological samples.

Quantification of CYP46A1 and CYP27A1 in Human Brain and Retina

Two fractions, the whole tissue homogenate and total membrane pellet after the 153 000*g* centrifugation of the tissue homogenate, were assayed (Tables 2 and 3). These fractions were tested because previously we were unable to detect the low abundance membrane protein CYP11A1 in the whole homogenate of bovine retina but could detect the protein in the total membrane pellet.[20] Similarly, in the present work, CYP46A1 was below the detection limit in the retinal homogenate, but it was possible to reliably measure CYP46A1 in the retinal total membrane pellet. In contrast, CYP27A1 could be quantified in both fractions, in both retina and brain. A comparison of the whole homogenate and total membrane pellet shows similar levels of each P450 in the two fractions, except for CYP46A1 in the retina. In the gray matter of the temporal lobe, CYP27A1 was in the range of 97–120 and 107–121 fmol/mg of tissue protein in the whole homogenate and total membrane pellet, respectively, whereas the range of CYP46A1 expression was about 3-fold higher (320–340 and 326–385 fmol/mg of tissue protein in the whole homogenate and total membrane pellet, respectively). In the retina, however, CYP27A1 turned out to be a much more abundant (≈6–10-fold) protein than CYP46A1, with concentrations of 403–510 and 464–570 fmol/mg of tissue protein in the whole homogenate and total membrane pellet, respectively. The retinal content of CYP46A1 was 58–63 fmol/mg of tissue protein in the total membrane pellet. Thus, in the present study we demonstrated the advantage of the "membrane pellet" approach[20] for the quantification of low abundance membrane proteins. The high-speed centrifugation which generates the total membrane pellet separates the membrane-associated P450s from the bulk of tissue soluble proteins and enriches the total membrane pellet with the P450 enzymes. This partially helps to overcome a broad dynamic range of cellular proteins, which is an obstacle for quantitative measurements. Assuming the average mass of tissue proteins is 50 kDa, 1 mg of tissue protein is equal to 20 nmoles. This

makes the dynamic range of the measurement on the total membrane pellet equal to 3.5×10^{-7} for CYP11A1 (≈ 7 fmol/20 nmoles of tissue protein[20]). Note that quantification using the total membrane pellet is possible only when the membrane proteins remain associated with the membrane during tissue homogenization and do not distribute between the supernatant and pellet after high speed centrifugation.[20] This is usually the case for microsomal P450s that have the N-terminal transmembrane anchor[30] and also seems to be the case for mitochondrial P450s, as demonstrated by our studies of CYP11A1 and CYP27A1. Unlike microsomal P450s, mitochondrial enzymes do not have the transmembrane anchor and interact with the lipid bilayer via several non-contiguous portions of the polypeptide chain.[31]

The quantification of other P450 enzymes by different methods has been reported, including drug-metabolizing P450s in the liver measured by semi-quantitative immunochemical staining[32] and LC-MS/MS[18] after separation of a microsomal fraction by the SDS-PAGE. The mean enzyme levels were in the range of 100–200 pmol of P450/mg microsomal protein. In our study, we were able to improve the limit of detection to 50 fmol/mg tissue protein and use a gel-free format by conducting the measurements in-solution in the presence of detergent and by using ^{15}N-labeled proteins as internal standards.

Quantification of Cholesterol Metabolites, the Products of CYP46A1 and CYP27A1

The same tissue samples used for the P450 measurements were used for the quantification of 24S-hydroxycholesterol, the product of enzymatic activities of CYP46A1; and two CYP27A1 metabolites, 27-hydroxycholesterol and 5-cholestenoic acid, that are formed in the brain and retina, respectively (Table 4). Higher expression of CYP46A1 was observed in the brain compared to the retina, and this corresponded to a higher concentration of 24S-hydroxycholesterol in the brain compared to the retina. Higher expression of CYP27A1 was observed in the retina compared to the brain, and this corresponded to higher concentrations of the associated metabolites in the retina compared to the brain. The concentrations of the cholesterol metabolites, however, varied among the donors and, on an individual basis, were not correlated with enzyme expression levels. We measured up to 5-fold inter-individual variability of 5-cholestenoic acid, corresponding to observations made previously[13], the levels of which did not correlate to the concentration of CYP27A1 in the respective individuals. In fact, the highest concentration of 5-cholestenoic acid was in the retina of donor 12, which had the lowest CYP27A1 expression; and donor 17, with the lowest concentration of 5-cholestenoic acid, had the highest expression of CYP27A1. Retinal levels of the CYP46A1 product 24S-hydroxycholesterol varied as well, but these were low pmol/mg protein amounts near the limit of sterol detection. At such low concentrations, definite conclusions regarding the CYP46A1-product relationship are not possible. In the gray matter of the temporal lobe, the concentration of the CYP27A1 product (27-hydroxycholesterol) had less inter-individual variability than the concentration of the product in the retina (5-cholestenoic acid) and seemed to correlate with the CYP27A1 expression levels on an individual basis. Donor 3 had the lowest 27-hydroxycholesterol content and the lowest CYP27A1 expression; donor 4 had intermediate metabolite and protein levels, and donor 2 had the highest content of both 27-hydroxycholesterol and CYP27A1 protein. Thus by comparing the enzyme and metabolite concentrations we were able to determine that in the retina, individuals' expression levels of CYP27A1 do not correlate with the corresponding metabolite concentrations.

The lack of enzyme-product correlation in the retina raises a question regarding the possible mechanism of decreased CYP27A1 activity in this organ, resulting in a lower metabolite formation. One cause could be a post-translational modification of the protein, resulting from the highly oxidative retinal environment and relatively high concentration of polyunsaturated fatty acids. Tables 2 and 3 show that measurements based on one peptide in

the retina, the lysine-containing VVLAPETGELK in CYP27A1, consistently resulted in lower CYP27A1 values. The retinal content of CYP27A1 was approximately 410 fmol/mg tissue protein based on this peptide alone, and approximately 517 fmol/mg tissue protein based on the other three peptides. In the brain, however, an underestimation of CYP27A1 based on the VVLAPETGELK peptide was not observed. This analysis implies that a post-translational modification of CYP27A1 may occur in the retina but not the brain. Experiments are in progress to test this hypothesis.

Conclusions

In the present study we have used the combination of MRM and GC-MS measurements to investigate the enzyme-product relationships. By quantifying two low abundance membrane proteins CYP27A1 and CYP46A1 in a gel-free format in the human brain and retina, we demonstrated the applicability of our previously developed MRM protocol for measurements of membrane proteins and generated data indicating important differences in cholesterol elimination from the retina as compared to that in the brain. Our results are consistent with the established role of CYP46A1 as the principal cholesterol hydroxylase in the brain[8] and support a greater role for CYP27A1 in cholesterol elimination from the retina. Subsequent quantification of the P450 metabolites by GC-MS enabled detection of the lost enzyme-product relationship in human retina but not human brain and created the basis for our current studies investigating the nature of this discrepancy. Collectively, our data demonstrate that the mechanism of cholesterol elimination from the retina is indeed different from that in the brain (cholesterol 27-hydroxylation *vs*. cholesterol 24-hydroxylation) and that simultaneous use of the advanced mass spectrometry techniques represents a powerful approach in studies of the enzyme-product relationship.

Supplementary Material

Refer to Web version on PubMed Central for supplementary material.

Acknowledgments

The authors thank Tonya Sims, Somier McLaughlin and the Cleveland Eye Bank for assistance in eye tissue acquisition, Dr. M. Shimoji for help in sample preparation, and Dr. I. Bederman for help in measuring the cholesterol metabolites. This work was supported in part by grants from the National Institutes of Health (EY018383 and AG024336 to I.A.P.) and postdoctoral research training fellowship T32 EY07157 from the Visual Sciences Training Program (to R.E.R). I.A.P is also a recipient of the Jules and Doris Stein Professorship from the Research to Prevent Blindness Foundation. Certain commercial materials, instruments, and equipment are identified in this manuscript in order to specify the experimental procedure as completely as possible. In no case does such identification imply a recommendation or endorsement by the National Institute of Standards and Technology (NIST) nor does it imply that the materials, instruments, or equipment identified are necessarily the best available for the purpose.

References

1. Third report of the National Cholesterol Education Program (NCEP) expert panel on detection, evaluation, and treatment of high blood cholesterol in adults (adult treatment panel III) final report. Circulation. 2002; 106:3143–3421. [PubMed: 12485966]
2. Wolozin B. Cholesterol and the biology of Alzheimer's disease. Neuron. 2004; 41:7–10. [PubMed: 14715130]
3. van Leeuwen R, Klaver CC, Vingerling JR, Hofman A, van Duijn CM, Stricker BH, de Jong PT. Cholesterol and age-related macular degeneration: is there a link? Am J Ophthalmol. 2004; 137:750–752. [PubMed: 15059717]
4. Pikuleva IA. Cholesterol-metabolizing cytochromes P450: implications for cholesterol lowering. Expert Opin Drug Metab Toxicol. 2008; 4:1403–1414. [PubMed: 18950282]

5. Lutjohann D, Breuer O, Ahlborg G, Nennesmo I, Siden A, Diczfalusy U, Bjorkhem I. Cholesterol homeostasis in human brain: evidence for an age-dependent flux of 24S-hydrohycholesterol from the brain into the circulation. Proc Natl Acad Sci USA. 1996; 93:9799–9804. [PubMed: 8790411]
6. Bjorkhem I, Lutjohann D, Diczfalusy U, Stahle L, Ahlborg G, Wahren J. Cholesterol homeostasis in human brain: turnover of 24S-hydroxycholesterol and evidence for a cerebral origin of most of this oxysterol in the circulation. J Lipid Res. 1998; 39:1594–1600. [PubMed: 9717719]
7. Lund EG, Guileyardo JM, Russell DW. cDNA cloning of cholesterol 24-hydroxylase, a mediator of cholesterol homeostasis in the brain. Proc Natl Acad Sci USA. 1999; 96:7238–7243. [PubMed: 10377398]
8. Bjorkhem I, Heverin M, Leoni V, Meaney S, Diczfalusy U. Oxysterols and Alzheimer's disease. Acta Neurol Scand. 2006; 114:43–49.
9. Tserentsoodol N, Sztein J, Campos M, Gordiyenko NV, Fariss RN, Lee JW, Fliesler SJ, Rodriguez IR. Uptake of cholesterol by the retina occurs primarily via a low density lipoprotein receptor-mediated process. Mol Vis. 2006; 12:1306–1318. [PubMed: 17110914]
10. Lee JW, Fuda H, Javitt NB, Strott CA, Rodriguez IR. Expression and localization of sterol 27-hydroxylase (CYP27A1) in monkey retina. Exp Eye Res. 2006; 83:465–469. [PubMed: 16549062]
11. Bretillon L, Diczfalusy U, Bjorkhem I, Maire MA, Martine L, Joffre C, Acar N, Bron A, Creuzot-Garcher C. Cholesterol-24S-hydroxylase (CYP46A1) is specifically expressed in neurons of the neural retina. Curr Eye Res. 2007; 32:361–366. [PubMed: 17453958]
12. Ramirez DMO, Andersson S, Russell DW. Neuronal expression and subcellular localization of cholesterol 24-hydroxylase in the mouse brain. J Comp Neurol. 2008; 507:1676–1693. [PubMed: 18241055]
13. Mast N, Reem R, Bederman I, Huang S, DiPatre PL, Bjorkhem I, Pikuleva IA. Cholestenoic acid is an important elimination product of cholesterol in the retina: comparison of retinal cholesterol metabolism to that in the brain. Invest Ophthalmol Vis Sci. (in press).
14. Anderson L, Hunter CL. Quantitative mass spectrometric multiple reaction monitoring assays for major plasma proteins. Mol Cell Proteomics. 2006; 5:573–588. [PubMed: 16332733]
15. Keshishian H, Addona T, Burgess M, Kuhn E, Carr SA. Quantitative, multiplexed assays for low abundance proteins in plasma by targeted mass spectrometry and stable isotope dilution. Mol Cell Proteomics. 2007; 6:2212–2229. [PubMed: 17939991]
16. Picotti P, Bodenmiller B, Mueller LN, Domon B, Aebersold R. Full dynamic range proteome analysis of *S. cerevisiae* by targeted proteomics. Cell. 2009; 138:795–806. [PubMed: 19664813]
17. Kitteringham NR, Jenkins RE, Lane CS, Elliott VL, Park BK. Multiple reaction monitoring for quantitative biomarker analysis in proteomics and metabolomics. J Chromatogr, B. 2009; 877:1229–1239.
18. Seibert C, Davidson BR, Fuller BJ, Patterson LH, Griffiths WJ, Wang Y. Multiple-approaches to the identification and quantification of cytochromes P450 in human liver tissue by mass spectrometry. J Proteome Res. 2009; 8:1672–1681. [PubMed: 19714871]
19. Jiang H, Ramos AA, Yao X. Targeted quantification of overexpressed and endogenous cystic fibrosis transmembrane conductance regulator using multiple reaction monitoring tandem mass spectrometry and oxygen stable isotope dilution. Anal Chem. 2010; 82:336–342. [PubMed: 19947594]
20. Liao WL, Heo GY, Dodder NG, Pikuleva IA, Turko IV. Optimizing the conditions of a multiple reaction monitoring assay for membrane proteins: quantification of cytochrome P450 11A1 and adrenodoxin reductase in bovine adrenal cortex and retina. Anal Chem. 2010; 82:5760–5767. [PubMed: 20521825]
21. Pikuleva IA, Bjorkhem I, Waterman MR. Expression, purification, and enzymatic properties of recombinant human cytochrome P450c27 (CYP27). Arch Biochem Biophys. 1997; 343:123–130. [PubMed: 9210654]
22. Mast N, Norcross R, Andersson U, Shou M, Nakayama K, Bjorkhem I, Pikuleva IA. Broad substrate specificity of human cytochrome P450 46A1 which initiates cholesterol degradation in the brain. Biochemistry. 2003; 42:14284–14292. [PubMed: 14640697]
23. Marley J, Lu M, Bracken C. A method for efficient isotopic labeling of recombinant proteins. J Biomol NMR. 2001; 20:71–75. [PubMed: 11430757]

24. Omura R, Sato R. The carbon monoxide-binding pigment of liver microsomes. I. Evidence for its hemoprotein nature. J Biol Chem. 1964; 239:2370–2378. [PubMed: 14209971]

25. Janecki DJ, Bemis KG, Tegeler TJ, Sanghani PC, Zhai L, Hurley TD, Bosron WF, Wang M. A multiple reaction monitoring method for absolute quantification of the human liver alcohol dehydrogenase ADH1C1 isoenzyme. Anal Biochem. 2007; 369:18–26. [PubMed: 17692277]

26. Brun V, Dupuis A, Adrait A, Marcellin M, Thomas D, Court M, Vandenesch F, Garin J. Isotope-labeled protein standards: toward absolute quantitative proteomics. Mol Cell Proteomics. 2007; 6:2139–2149. [PubMed: 17848587]

27. Singh R, Crow FW, Babic N, Lutz WH, Lieske JC, Larson TS, Kumar R. A liquid chromatography-mass spectrometry method for the quantification of urinary albumin using a novel ^{15}N-isotopically labeled albumin internal standard. Clin Chem. 2007; 53:540–542. [PubMed: 17327509]

28. Pikuleva IA, Mast N, Liao WL, Turko IV. Studies of membrane topology of mitochondrial cholesterol hydroxylases CYPs 27A1 and 11A1. Lipids. 2008; 43:1127–1132. [PubMed: 18791760]

29. Mast N, Liao WL, Pikuleva IA, Turko IV. Combined use of mass spectrometry and heterologous expression for identification of membrane-interacting peptides in cytochrome P450 46A1 and NADPH-cytochrome P450 oxidoreductase. Arch Biochem Biophys. 2009; 483:81–89. [PubMed: 19161969]

30. von Wachenfeldt, C.; Johnson, EF. Structures of eukaryotic cytochrome P450 enzymes. In: Ortiz de Montellano, PR., editor. Cytochrome P450: Structure, Mechanism, and Biochemistry. Plenum Press; New York: 1995. p. 183-244.

31. Omura T. Mitochondrial P450s. Chemico-Biological Interactions. 2006; 163:86–93. [PubMed: 16884708]

32. Guengerich FP, Turvy CG. Comparison of levels of several human microsomal cytochrome P-450 enzymes and epoxide hydrolase in normal and disease states using immunochemical analysis of surgical liver samples. J Pharmacol Exp Ther. 1991; 256:1189–1194. [PubMed: 2005581]

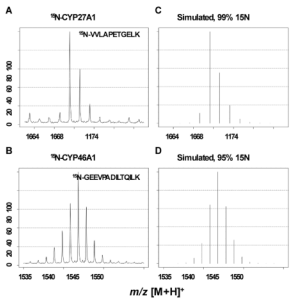

Figure 1.

Experimental and simulated MALDI mass spectra of representative peptides from ^{15}N-labeled P450s. (A) ^{15}N-VVLAPETGELK from ^{15}N-CYP27A1; the labeling incorporation was determined to be 99% when compared to the simulated spectrum (C). Similarly, (B) ^{15}N-GEEVPADILTQILK from ^{15}N-CYP46A1; the labeling incorporation was determined to be 95% when compared to the simulated spectrum (D).

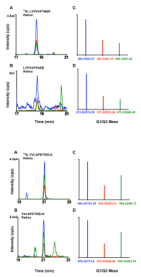

Figure 2.
Extracted ion chromatograms (A – B) and MRM spectra (C – D) of transitions monitored for ^{15}N-CYP27A1 and CYP27A1 in the retina. Data are presented for the LYPVVPTNSR and VVLAPETGELK peptides. Overlaid extracted ion chromatograms and ions in the MRM/MS spectra are color-coordinated (cps, counts per second).

Table 1

Peptides and MRM transitions used for the quantification of CYP27A1 and CYP46A1.

	MRM transitions (*m/z*)			
	Q1(charge)		**Q3(type, charge)**	
CYP27A1				
LYPVVPTNSR	573.32 (+2)	574.29 (y^5, +1)	673.36 (y^6, +1)	869.48 (y^8, +1)
^{15}N- LYPVVPTNSR	580.30 (+2)	583.27 (y^5, +1)	683.33 (y^6, +1)	881.45 (y^8, +1)
EIEVDGFLFPK	647.34 (+2)	708.41 (y^6, +1)	823.43 (y^7, +1)	922.00 (y^8, +1)
^{15}N- EIEVDGFLFPK	653.32 (+2)	715.39 (y^6, +1)	831.41 (y^7, +1)	931.48 (y^8, +1)
IQHPFGSVPFGYGVR	554.29 (+3)	551.29 (y^5, +1)	698.36 (y^6, +1)	795.41 (y^7, +1)
^{15}N- IQHPFGSVPFGYGVR	561.27 (+3)	559.27 (y^5, +1)	707.34 (y^6, +1)	805.39 (y^7, +1)
VVLAPETGELK	578.33 (+2)	773.40 (y^7, +1)	844.44 (y^8, +1)	957.53 (y^9, +1)
^{15}N- VVLAPETGELK	584.32 (+2)	781.38 (y^7, +1)	853.41 (y^8, +1)	967.50 (y^9, +1)
CYP46A1				
VLQDVFLDWAK	667.36 (+2)	779.41 (y^6, +1)	993.50 (y^8, +1)	1121.56 (y^9, +1)
^{15}N- VLQDVFLDWAK	674.34 (+2)	787.38 (y^6, +1)	1003.47 (y^8, +1)	1133.53 (y^9, +1)
TSVIVTSPESVK	623.85 (+2)	747.39 (y^7, +1)	846.46 (y^8, +1)	959.54 (y^9, +1)
^{15}N- TSVIVTSPESVK	630.33 (+2)	755.36 (y^7, +1)	855.43 (y^8, +1)	969.51 (y^9, +1)
GEEVPADILTQILK	509.29 (+3)	556.34 (y^{10}, +2)	602.39 (y^5, +1)	715.47 (y^7, +1)
^{15}N- GEEVPADILTQILK	514.61 (+3)	562.32 (y^{10}, +2)	609.37 (y^5, +1)	723.45 (y^7, +1)
LLEEETLIDGVR	693.88 (+2)	773.45 (y^7, +1)	1031.54 (y^9, +1)	1160.58 (y^{10}, +1)
^{15}N- LLEEETLIDGVR	701.35 (+2)	783.42 (y^7, +1)	1043.5 (y^9, +1)	1173.54 (y^{10}, +1)

Table 2

Quantification of CYP27A1 and CYP46A1 in Human Temporal Lobe Whole Homogenate and Total Membrane Pellet[a]

protein (fmol/mg tissue protein)[b]								
	homogenate				pellet			
Patient ID	***#1***	***#2***	***#3***	***#4***	***#1***	***#2***	***#3***	***#4***
CYP27A1								
LYPVVPTNSR	111 ± 12	110 ± 10	90 ± 18	100 ± 14	124 ± 25	101 ± 10	105 ± 19	103 ± 10
VVLAPETGELK	83 ± 10	111 ± 13	104 ± 10	140 ± 14	117 ± 10	132 ± 10	109 ± 16	124 ± 20
consensus	**97 ± 12**	**111 ± 13**	**97 ± 15**	**120 ± 15**	**121 ± 19**	**117 ± 11**	**107 ± 19**	**114 ± 16**
average	**110 ± 16**							
CYP46A1								
TSVIVTSPESVK	309 ± 12	328 ± 29	330 ± 10	349 ± 10	410 ± 30	341 ± 26	450 ± 30	437 ±27
LLEEETLIDGVR	307 ± 35	332 ± 53	342 ± 51	291 ± 31	366 ± 40	302 ± 10	415 ± 44	343 ± 38
VLQDVFLDWAK	315 ± 86	365 ± 69	328 ± 72	338 ± 30	378 ± 31	343 ± 56	360 ± 10	266 ± 32
GEEVPADILTQILK	347 ± 40	334 ± 24	320 ± 30	322 ± 57	385 ± 47	317 ± 33	300 ± 40	378 ± 19
consensus	**320 ± 49**	**340 ± 51**	**330 ± 54**	**325 ± 38**	**385 ± 45**	**326 ± 35**	**381 ± 37**	**356 ± 34**
average	**345 ± 46**							

[a] Whole tissue homogenate was centrifuged at 153 000*g* for 30 min to generate the total membrane pellet.

[b] The concentration was calculated for three experimental replicates by monitoring three transitions per individual peptide and presented as mean ± SD. For the consensus, the data for two peptides from CYP27A1 and for four peptides from CYP46A1 were combined and presented as mean ± SD. For the average, the data for the whole tissue homogenate and total membrane pellet were combined and presented as mean ± SD. The monitored transitions are summarized in Table 1.

Table 3

Quantification of CYP27A1 and CYP46A1 in Human Retina Whole Homogenate and Total Membrane Pellet[a]

protein (fmol/mg tissue protein)[b]								
	homogenate				pellet			
Patient ID	***#12***	***#13***	***#17***	***#20***	***#12***	***#13***	***#17***	***#20***
CYP27A1								
LYPVVPTNSR	440 ± 130	690 ± 160	590 ± 140	520 ± 100	514 ± 55	532 ± 88	647 ± 20	665 ± 112
VVLAPETGELK	310 ± 60	350 ± 60	390 ± 30	390 ± 100	400 ± 16	475 ± 15	501 ± 52	464 ± 19
IQHPFGSVPFGYGVR	340 ± 40	490 ± 45	450 ± 50	420 ± 20	426 ± 16	480 ± 24	540 ± 60	464 ± 23
EIEVDGFLFPK	520 ± 40	510 ± 50	480 ± 40	490 ± 70	517 ± 29	550 ± 40	590 ± 34	537 ± 54
consensus	**403 ± 80**	**510 ± 92**	**480 ± 73**	**455 ± 78**	**464 ± 38**	**509 ± 51**	**570 ± 51**	**533 ± 63**
average	**490 ± 71**							
CYP46A1								
LLEEETLIDGVR	ND	ND	ND	ND	60 ± 9	60 ± 2	69 ± 3	58 ± 4
VLQDVFLDWAK	ND	ND	ND	ND	58 ± 3	60 ± 8	65 ± 5	63 ± 3
GEEVPADILTQILK	ND	ND	ND	ND	55 ± 5	57 ± 2	56 ± 3	55 ± 7
consensus					**58 ± 7**	**59 ± 5**	**63 ± 5**	**59 ± 6**
average	**60 ± 7**							

[a] Whole tissue homogenate was centrifuged at 153 000*g* for 30 min to generate the total membrane pellet.

[b] The concentration was calculated for three experimental replicates by monitoring three transitions per individual peptide and presented as mean ± SD. For the consensus, the data for four peptides from CYP27A1 and for three peptides from CYP46A1 were combined and presented as mean ± SD. For the average, the data for the whole tissue homogenate and total membrane pellet were combined and presented as mean ± SD. ND, not detected. The monitored transitions are summarized in Table 1.

Table 4

Quantification of cholesterol metabolites, the products of CYP46A1 and CYP27A1. Protein concentrations of the P450s are given for comparison.

Donor	Temporal Lobe Gray Matter				Retina				
	24S-Hydroxy-cholesterol, pmol/mg protein[a]	CYP46A1, fmol/mg protein[b]	27-Hydroxy-cholesterol, pmol/mg protein[a]	CYP27A1, fmol/mg tissue protein[b]	Donor	24S-Hydroxy-cholesterol, pmol/mg protein[c]	CYP46A1, fmol/mg protein[d]	5-Cholest-enoic acid, pmol/mg protein[c]	CYP27A1, fmol/mg protein[d]
#1	ND[e]	385 ± 45	ND	121 ± 19	#12	4	58 ± 7	130	464 ± 38
#2	1,294 ± 42	326 ± 35	22 ± 1	117 ± 11	#13	1	59 ± 5	29	509 ± 51
#3	1,160 ± 56	381 ± 37	11 ± 1	107 ± 19	#17	2	63 ± 5	25	570 ± 51
#4	1,339 ± 45	356 ± 34	14 ± 1	114 ± 16	#20	3	59 ± 6	51	533 ± 63

[a] Taken from reference 13, three extracts from the same tissue were analyzed. The results represent mean ± SD.

[b] Taken from Table 2

[c] A single extract was used to quantify the metabolite, represents a new measurement conducted on a different donor as compared to the study in reference 13

[d] Taken from Table 3

[e] ND, not determined